

## Driving the Gaseous Evolution of Massive Galaxies in the Early Universe

Dominik A. Riechers<sup>1</sup>

<sup>1</sup>*California Institute of Technology, 1200 East California Blvd, MC 249-17, Pasadena, CA 91125, USA*

**Abstract.** Studies of the molecular interstellar medium that fuels star formation and supermassive black hole growth in galaxies at cosmological distances have undergone tremendous progress over the past few years. Based on the detection of molecular gas in  $>120$  galaxies at  $z=1$  to 6.4, we have obtained detailed insight on how the amount and physical properties of this material in a galaxy are connected to its current star formation rate over a range of galaxy populations. Studies of the gas dynamics and morphology at high spatial resolution allow us to distinguish between gas-rich mergers in different stages along the “merger sequence” and disk galaxies. Observations of the most massive gas-rich starburst galaxies out to  $z>5$  provide insight into the role of cosmic environment for the early growth of present-day massive spheroidal galaxies. Large-area submillimeter surveys have revealed a rare population of extremely far-infrared-luminous gas-rich high-redshift objects, which is dominated by strongly lensed, massive starburst galaxies. These discoveries have greatly improved our understanding of the role of molecular gas in the evolution of massive galaxies through cosmic time.

### 1. Introduction

Great progress has been made in studies of galaxy evolution out to high redshift over the past years, but there are a number of fundamental questions that remain to be answered. One of the most important remaining issues is to understand whether star formation and the subsequent buildup of stellar mass in galaxies at early cosmic times occurs dominantly through major mergers (e.g., Springel et al. 2005) or through a combination of minor mergers and steady, so-called “cold-mode” accretion (e.g., Dekel et al. 2009). This issue is closely connected to the question how galaxies obtain the (dominantly molecular) gas that fuels star formation, and what their gas mass fractions are. Gas mass fractions, in relation to star formation rates, determine the evolutionary state of a galaxy (e.g., Daddi et al. 2010a; Tacconi et al. 2010). Next to these more general issues, it is important to better understand the physical properties, chemical composition, and dynamics of the star-forming gas in high- $z$  galaxies, which set the initial conditions for star formation (e.g., Riechers et al. 2006a, 2008a; Weiß et al. 2007).

All of these fundamental issues are directly tied to studies of molecular gas in high redshift galaxies. Despite the great progress that has been made in this field over the past 15 years, our understanding was ultimately limited by the technical capabilities of past observatories in the centimeter to submillimeter wavelength range, where the most common molecular gas diagnostics can be observed at high redshift. New observatories, such as the Atacama Large sub/Millimeter Array (ALMA) that currently

nears completion, will be key to ultimately solve many of the remaining mysteries in this field. This article summarizes some of the most recent (pre-ALMA) progress in the field of molecular gas observations out to high redshift, and how the gas properties entangle with the driving mechanism of star formation in massive high redshift galaxies.

## 2. CO Detections at High Redshift: a Brief Summary

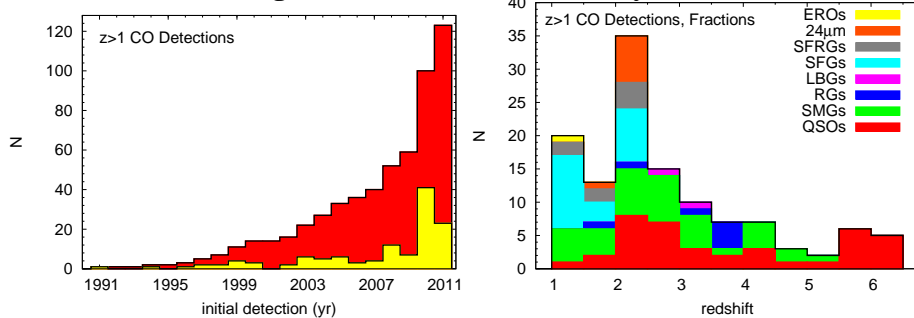


Figure 1. Detections of CO emission in  $z > 1$  galaxies. *Left*: Total number of detections (red) and detections per year (yellow) since the initial detection in 1991/1992. *Right*: Detections as of December 2011 as a function of redshift, and color encoded by galaxy type (figure updated from Riechers 2011a).

To date, molecular gas (most commonly CO) has been detected in  $>120$  galaxies at  $z > 1$  (see reviews by Solomon & Vanden Bout 2005; Omont 2007; Fig. 1), back to only 870 million years after the Big Bang (corresponding to  $z=6.42$ ; e.g., Walter et al. 2003, 2004; Bertoldi et al. 2003; Riechers et al. 2009). The bulk of these galaxies are massive, hosting molecular gas reservoirs of  $M_{\text{gas}} > 10^{10} M_{\odot}$ , commonly with high gas fractions of (at least) tens of per cent. The sensitivity of past observatories has only allowed us to probe less massive and/or less gas-rich systems with the aid of strong gravitational lensing (e.g., Baker et al. 2004; Coppin et al. 2007; Riechers et al. 2010a, 2011a; Swinbank et al. 2010, 2011).

Approximately 20% of the detected systems are massive, gas-rich optically/near-infrared selected star forming galaxies (SFGs; e.g., Daddi et al. 2010a; Tacconi et al. 2010), and 30% each are far-infrared-luminous, star-bursting quasars (QSOs; e.g., Wang et al. 2010; Riechers 2011b) and submillimeter galaxies (SMGs; e.g., Greve et al. 2005; Tacconi et al. 2008; Fig. 1). The rest of CO-detected high-redshift galaxies are limited samples of galaxies selected through a variety of techniques, such as Extremely Red Objects (EROs), Star-Forming Radio-selected Galaxies (SFRGs),  $24 \mu\text{m}$ -selected galaxies, gravitationally lensed Lyman-break galaxies (LBGs), and radio galaxies (RGs; see Riechers 2011a for a recent summary).

Besides CO, the high-density gas tracers HCN,  $\text{HCO}^+$ , HNC, CN, and  $\text{H}_2\text{O}$  were detected towards a small subsample of these galaxies (e.g., Solomon et al. 2003; Riechers et al. 2006b, 2007, 2010b, 2011b; Guélin et al. 2007; Omont et al. 2011).

## 3. Luminosity Relations and the Star Formation Law

The CO luminosity  $L'_{\text{CO}}$  is commonly considered to be a measure for the total molecular gas mass  $M_{\text{gas}}$  in galaxies, and the far-infrared (FIR) luminosity  $L_{\text{FIR}}$  is considered to be a measure for the star formation rate (SFR; e.g., Solomon & Vanden Bout 2005). Thus, the relation between  $L'_{\text{CO}}$  or  $M_{\text{gas}}$  and  $L_{\text{FIR}}$  or SFR may be considered a spatially

integrated version of the Schmidt-Kennicutt “star formation law” between gas surface density and star formation rate surface density (e.g., Kennicutt 1998).

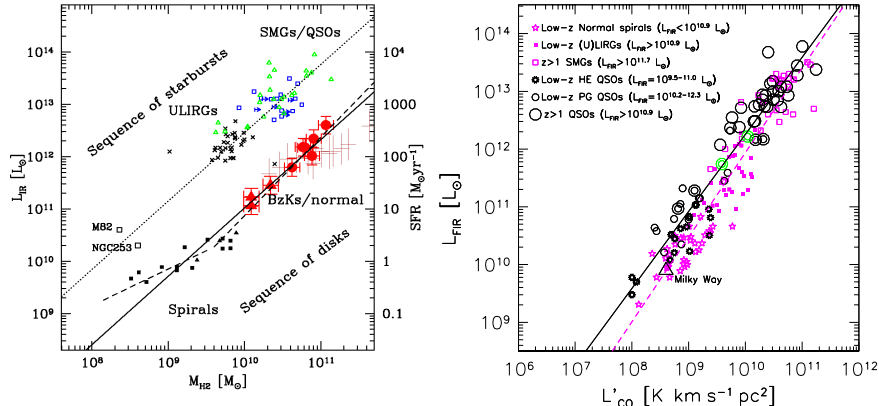


Figure 2. Comparison of CO luminosity/gas mass with (far-) infrared luminosity as a tracer of the star formation rate in low- and high- $z$  galaxies. *Left:*  $M_{\text{gas}}-L_{\text{IR}}$  relation for low- $z$  spirals, starbursts and ULIRGs, and high- $z$  SFGs (“BzKs/normal”), SMGs, and quasars. The solid line represents a fit to spiral galaxies and SFGs, and the dotted line shows the same trend offset by 1.1 dex in  $L_{\text{IR}}$  (which is consistent with the starburst galaxies, ULIRGs, SMGs and quasars). These two lines may represent two sequences for disk and starburst galaxies, with the offset being due to different dynamical timescales for star formation (e.g., Daddi et al. 2010b). *Right:*  $L'_{\text{CO}}-L_{\text{FIR}}$  relation for quasars at low and high  $z$  (fitted by the solid line), and galaxies without dominant AGN at low  $z$  (spirals and (U)LIRGs) and at high  $z$  (SMGs; fitted by the dashed line). At high  $L'_{\text{CO}}$ , galaxies with and without dominant AGN statistically occupy the same region, while at low  $L'_{\text{CO}}$ , there is tentative evidence for an offset of quasars toward higher  $L_{\text{FIR}}$ . This may indicate that AGN heating contributes significantly to  $L_{\text{FIR}}$  at low  $L'_{\text{CO}}$ , but not at high  $L'_{\text{CO}}$  (Riechers 2011b).

Even in galaxies with luminous active galactic nuclei (AGN),  $L_{\text{FIR}}$  is commonly used as a proxy for the star formation rate in the host galaxy. In principle, both the AGN and star formation can heat the dust that gives rise to the continuum flux observed in the FIR, but the characteristic dust temperatures of AGN heating are typically by a factor of a few higher than those of dust heated by young stars. Thus, the warm dust in AGN-starburst systems observed in the rest-frame FIR is commonly thought to be dominated by heating within the host galaxy, in particular in the most intense, dust-enshrouded starbursts. If, however,  $L_{\text{FIR}}$  were to be dominated by the AGN, one would expect an elevated  $L_{\text{FIR}}$  for such galaxies in the  $L'_{\text{CO}}-L_{\text{FIR}}$  relation. In Figure 2 (right panel), a comparison of the  $L'_{\text{CO}}-L_{\text{FIR}}$  relation for nearby and high- $z$  quasars to nearby galaxies, (ultra-)luminous infrared galaxies ((U)LIRGs) and SMGs without dominant AGN is shown (Riechers 2011b). For galaxies with low  $L'_{\text{CO}}$ , there is an indication for an excess in  $L_{\text{FIR}}$  for quasars relative to other systems; however, there is no evidence for such a trend at high  $L'_{\text{CO}}$ . This may suggest that, in systems with relatively low gas and dust content, AGN contribute significantly to  $L_{\text{FIR}}$ , but not in systems with high gas and dust content. Thus, for massive high-redshift galaxies,  $L_{\text{FIR}}$  appears to be a good proxy for the SFR, even in quasars (Riechers 2011b).

Beyond the issue of dust heating, the question occurs if star formation progresses the same way in all types of galaxies. In disk-like spiral galaxies like the Milky Way, star formation takes place in molecular clouds with compact, dense cores, confined by self gravity (e.g., Solomon et al. 1987). In mergers, such as the Antennae

(NGC 4038/39; Fig. 3), the gas and star formation appear to peak on the galaxy nuclei, but also on relatively large scales in the dense overlap region between the merging galaxies, leading to the formation of so-called super star clusters (e.g., Wilson et al. 2003). Such constellations are also commonly found in the highest-resolution CO studies of high-redshift FIR-luminous massive galaxies (Fig. 3; e.g., Riechers et al. 2008a, 2008b). In the nuclei of ULIRGs, the most extreme nearby starbursts, star formation appears to occur in a dense, intercloud medium, bound by the potential of the galaxy, rather than in virialized clouds (e.g., Downes & Solomon 1998). The differences between starburst and disk galaxies are reflected in the star formation law. When comparing the  $M_{\text{gas}}-L_{\text{IR}}$  relation for three largest CO-detected samples at high  $z$ , i.e., quasars, SMGs, and SFGs, to low redshift galaxies, two interesting trends occur. First, SFGs extend the relation found for nearby spiral galaxies to higher  $M_{\text{gas}}$ . Second, quasars and SMGs extend the trend found for the most intense nearby starbursts and ULIRGs to higher  $M_{\text{gas}}$ . Both trends agree with the same slope, but are offset by 1.1dex in  $L_{\text{IR}}$ . Daddi et al. (2010b) interpret this as evidence for two sequences in this relation for disk galaxies and starbursts, which emerge from the different dynamical timescales of star formation in these systems (Fig. 2, left; see also Genzel et al. 2010). Recent theoretical studies have attempted to understand the different trends based on the underlying conversion factor,  $\alpha_{\text{CO}}$ , from  $L'_{\text{CO}}$  to  $M_{\text{gas}}$ , and find that the two sequences could only be unified to a single relation when assuming a broad continuum of conversion factors (e.g., Narayanan 2012, this volume).

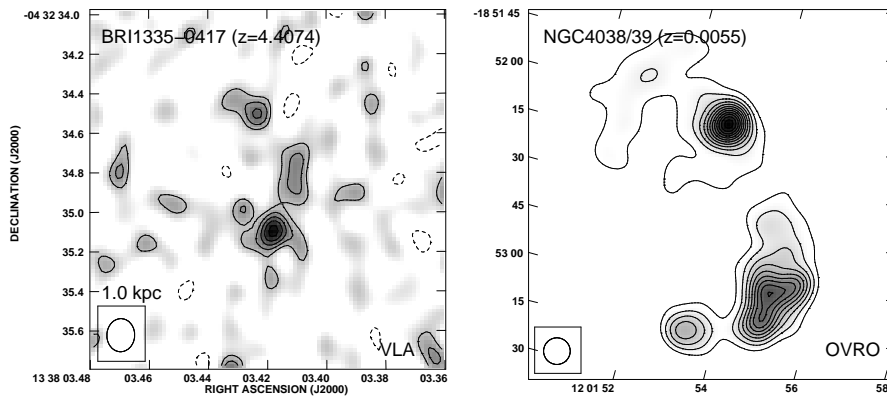


Figure 3. Molecular gas distribution in major mergers. *Left:* The  $z=4.41$  AGN-starburst system BRI 1335-0417 ( $0.16'' \times 0.14''$  resolution, corresponding to 1.0 kpc; Riechers et al. 2008a). *Right:* The nearby major merger NGC 4038/39 (the Antennae; convolved to 1.0 kpc resolution and rotated for illustration; Wilson et al. 2003). Both systems are dominated by a clumpy, asymmetric gas distribution, and some diffuse emission is seen at low flux density level. It is plausible to assume that the clumps can be identified with two galaxy nuclei and a dense overlap region in both cases.

#### 4. Gas Dynamics: A “Merger Sequence” of High Redshift Galaxies

The advent of the Expanded Very Large Array (EVLA)<sup>1</sup> has recently enabled studies of the full gas content, distribution and dynamics of different populations of high-redshift galaxies through observations of CO( $J=1 \rightarrow 0$ ) emission (e.g., Riechers et al. 2010a,

<sup>1</sup>The Expanded Very Large Array was recently re-named to the Jansky VLA.

2011c, 2011d, 2011e; Ivison et al. 2011). In contrast to previous studies at shorter wavelengths in higher rotational lines of CO, observations of CO  $J=1\rightarrow 0$  trace the full amount and extent of the molecular gas, and can be more directly compared to observations in the nearby universe, which are most commonly undertaken in CO  $J=1\rightarrow 0$ .

One particular aspect of these studies is that they provide deeper insight into the mechanisms that are driving the conversion of gas into stellar mass in the most intensely star-forming galaxies at early cosmic times, such as SMGs. It has been argued in the past that most SMGs are major mergers of two gas-rich galaxies (e.g., Tacconi et al. 2008; Engel et al. 2010). Detailed studies of CO ( $J=1\rightarrow 0$ ) emission with the EVLA confirm this picture, and show a range in merger properties and stages (e.g., Riechers et al. 2011c, 2011d; Fig. 4). Indeed, it becomes possible to place SMGs along a “merger sequence” of high redshift galaxies, ranging from systems with two disk-like gas-rich galaxies that are separated by tens of kiloparsec in projection and several hundreds  $\text{km s}^{-1}$  in velocity over actively merging systems with a single, morphologically and dynamically complex gas distribution to systems that have almost reached coalescence. These early investigations demonstrate that studies of larger samples at higher spatial resolution with the fully upgraded EVLA in the future will allow us to distinguish between different galaxy populations based on the physical properties of their interstellar media. This will yield a more complete understanding of the processes that trigger star formation and black hole activity in the early universe, and their relative importance for the buildup of stellar mass in galaxies as seen at present day.

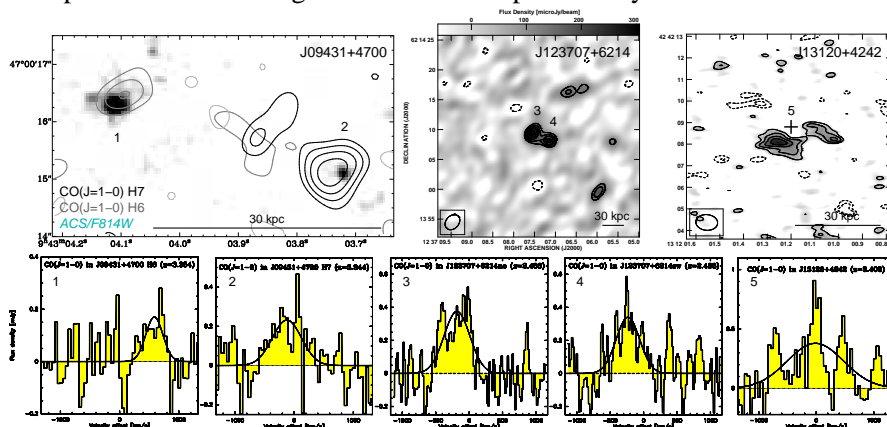


Figure 4. CO ( $J=1\rightarrow 0$ ) observations of submillimeter galaxies along the “merger sequence” with the Expanded Very Large Array (Riechers et al. 2011c, 2011d). SMGs show complex gas morphologies that can extend over  $>10$  kpc scales, and commonly consist of multiple components. The gas distribution and kinematics of the majority of SMGs are as expected for major, gas-rich mergers. The observed diversity in these properties is consistent with different merger stages, as shown here for three examples. *Left*: The two gas-rich galaxies in this SMG are separated by tens of kpc and  $\sim 700 \text{ km s}^{-1}$ , representing an early merger stage. *Middle*: This SMG still shows two separated components, but at similar velocity, representing a more advanced merger stage. *Right*: This SMG shows a single, complex extended gas structure with multiple velocity components, representing a fairly late merger stage.

## 5. Cosmic Environments of Massive Starbursts at Very High Redshift

Recent studies have led to the discovery of the long sought-after high-redshift tail of SMGs at  $z>4$  (e.g., Capak et al. 2008; Daddi et al. 2009). SMGs at the highest redshifts

are of particular interest, as they trace some of the most massive and active systems at early cosmic times. In cosmological simulations, such systems are expected to grow in the rare, most overdense regions in the early universe (e.g., Springel et al. 2005). Thus, very high- $z$  SMGs may trace the most distant proto-cluster regions in the universe, which have the potential to grow into the most massive cosmic structures seen at present day. Indeed, following the discovery of a SMG at an unprecedented redshift of  $z=5.298$ , observational evidence has recently been found for this mode of structure formation in the early universe (Capak et al. 2011; Riechers et al. 2010c; Fig. 5). Deep imaging and spectroscopy of its cosmic environment as part of the Cosmic Evolution Survey (COSMOS) reveals a high overdensity of Lyman-break galaxies at similar redshifts within a co-moving volume of 2 Mpc radius around the SMG. The structure of the central proto-cluster encompasses a halo mass of  $>4 \times 10^{11} M_{\odot}$ , which would be consistent with what is expected for the early formation of a present-day galaxy cluster. Clearly, future discovery and studies of SMGs at comparable and higher redshifts are desirable to determine the fraction of the first massive starbursts that are associated with such galaxy overdensities, as necessary to study the effects of environment on galaxy formation within a more general cosmological context.

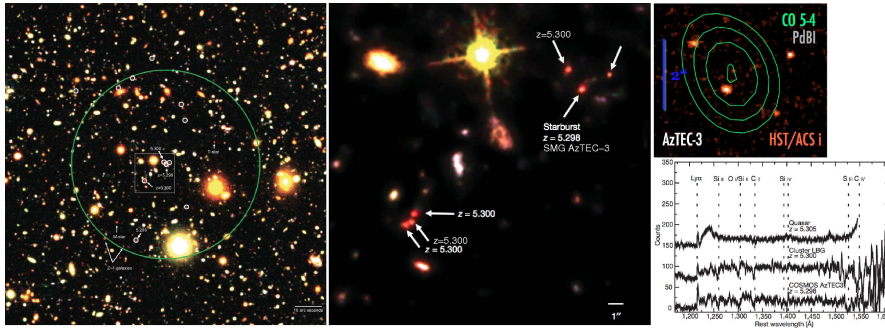


Figure 5. Gas properties and environment of the most distant SMG AzTEC-3 at  $z=5.298$  (Riechers et al. 2010c; Capak et al. 2011). *Left*:  $2' \times 2'$  region around AzTEC-3. The white circles show photometrically identified candidate Lyman-break galaxies (LBGs) at  $z=5.3$ , and the green circle indicates a region of 2 Mpc co-moving radius. The labels indicate spectroscopic redshifts of confirmed LBGs or of low- $z$  galaxies and stars rejected based on their spectral energy distributions. *Middle*: Zoom-in of the central 0.865 Mpc (co-moving) region, with spectroscopic redshifts labeled. *Right*: Zoom-in of the SMG, with CO( $J=5 \rightarrow 4$ ) contours overlaid (*top*), and optical spectra of the SMG and companion galaxies (*bottom*). The massive, very high  $z$  starburst galaxy AzTEC-3 traces a “proto-cluster” region of high galaxy overdensity in the early universe, showing that the highest-redshift SMGs may be an ideal tracer of the most massive cosmic structures at early cosmic times.

## 6. Herschel: The Lensing Revolution

One of the most intriguing recent discoveries made by the *Herschel Space Observatory* is the identification of a rare population of extremely luminous high-redshift starburst galaxies at submillimeter wavelengths ( $S_{500\mu\text{m}} > 100 \text{ mJy}$ ; e.g., Negrello et al. 2010). This population far exceeds the expected number counts of SMGs at the bright end, and is dominated by gravitationally lensed SMGs. This discovery is interesting, because it allows for a very efficient selection of gravitational lenses based on a flux density measurement alone (after rejection of low-redshift contaminants). Also, the natural magnification in size and flux density provided by gravitational lensing have enabled new

techniques to better understand the SMG population itself. First, the high expected CO emission line fluxes, paired with recent spectral bandwidth upgrades of radio/millimeter observatories, have yielded a significant number of “blind” CO detections in these and similar sources without any prior constraints on their redshifts (e.g., Riechers 2011b; Frayer et al. 2011; Cox et al. 2011; Harris et al. 2012; Lupu et al. 2012). Second, high-resolution CO imaging studies, in combination with detailed lens modeling, allow us to probe down to structure sizes that would remain inaccessible with current-generation instruments without the aid of gravitational lensing (e.g., Fig. 6; Riechers et al. 2011a; Swinbank et al. 2011; see also Riechers et al. 2008a). Only ALMA will match the sensitivity and resolution of these studies in unlensed galaxies, and will even allow us to probe down to individual molecular cloud scales in lensed systems.

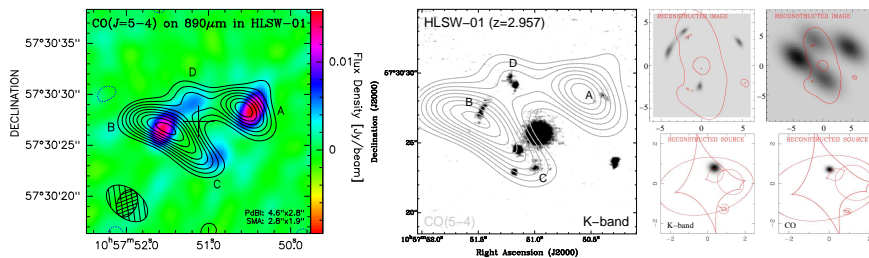


Figure 6. Multi-wavelength observations and modeling of HLSW-01, a rare, exceptionally bright, lensed SMG at  $z=2.957$  discovered in the HerMES *Herschel*/SPIRE survey (Riechers et al. 2011a; Gavazzi et al. 2011). *Left*: Overlay of CO( $J=5\rightarrow 4$ ) contours on observed-frame  $890\ \mu\text{m}$  continuum emission. A to D label the lensed images of the galaxy. *Middle*: Same overlaid on a  $2.2\ \mu\text{m}$  image. *Right*: Lens model of the  $2.2\ \mu\text{m}$  (*left*) and CO( $J=5\rightarrow 4$ ) emission (*right*) in the image (*top*) and source (*bottom*) planes. This SMG is lensed by a galaxy group at  $z\approx 0.6$ , yielding an extreme apparent  $250\ \mu\text{m}$  flux density of  $425\pm 10\ \text{mJy}$  due to a lensing magnification factor of  $\sim 10.9$ , and a wide lens image separation of  $\sim 9''$ . This source represents the bright end of a new population of lensed SMGs discovered with *Herschel*.

## 7. Summary and Outlook

Studies of the molecular interstellar medium in galaxies at cosmological distances have shown great progress in the past few years. These advances were possible due to a combination of improved selection techniques to identify gas-rich galaxies in the early universe and major improvements in instrumentation, which have enabled studies of less extreme galaxy populations than previously possible, and have liberated high redshift molecular line studies from the prerequisite of a precise spectroscopic redshift obtained through other measures (which were a major selection bias in the past). The most recent studies thus finally probe beyond the “tip of the iceberg” of the most far-infrared-luminous galaxies with optical spectroscopic redshifts that were the focus of molecular line studies at high  $z$  in the past. These observations also offer a “sneak peek” into the detailed investigations of the physical properties of galaxies at early cosmic times that will become possible with ALMA, once it commences full science operations.

**Acknowledgments.** I would like to thank the organizers of “Galaxy Mergers in an Evolving Universe” for the invitation to this diverse and stimulating conference. Also, I would like to thank my collaborators on studies related to this subject, in particular Frank Bertoldi, Peter Capak, Chris Carilli, Asantha Cooray, Pierre Cox, Emanuele Daddi, Roberto Neri, Nick Scoville, Fabian Walter, and Ran Wang. I acknowledge support from NASA through a *Spitzer Space Telescope* grant.

**References**

- Baker, A. J., Tacconi, L. J., Genzel, R., Lehnert, M. D., & Lutz, D. 2004, *ApJ*, 604, 125  
Bertoldi, F., et al. 2003, *A&A*, 409, L47  
Capak, P. L., et al. 2008, *ApJ*, 681, L53  
Capak, P. L., et al. 2011, *Nature*, 470, 233  
Coppin, K. E. K., et al. 2007, *ApJ*, 665, 936  
Cox, P., et al. 2011, *ApJ*, 740, 63  
Daddi, E., et al. 2009, *ApJ*, 694, 1517  
Daddi, E., et al. 2010a, *ApJ*, 713, 686  
Daddi, E., et al. 2010b, *ApJ*, 714, L118  
Dekel, A., et al. 2009, *Nature*, 457, 451  
Downes, D., & Solomon, P. M. 1998, *ApJ*, 507, 615  
Engel, H., et al. 2010, *ApJ*, 724, 233  
Frayser, D. T., et al. 2011, *ApJ*, 726, L22  
Gavazzi, R., et al. 2011, *ApJ*, 738, 125  
Genzel, R., et al. 2010, *MNRAS*, 407, 2091  
Greve, T. R., et al. 2005, *MNRAS*, 359, 1165  
Guelin, M., et al. 2007, *A&A*, 462, L45  
Harris, A. I., et al. 2012, *ApJ*, submitted  
Ivison, R. J., et al. 2011, *MNRAS*, 412, 1913  
Kennicutt, R. C., Jr. 1998, *ApJ*, 498, 541  
Lupu, R. E., et al. 2012, *ApJ*, submitted (arXiv:1009.5983)  
Narayanan, D. 2012, *ASPC*, this volume  
Negrello, M., et al. 2010, *Science*, 330, 800  
Omont, A. 2007, *RPPh*, 70, 1099  
Omont, A., et al. 2011, *A&A*, 530, L3  
Riechers, D. A., et al. 2006a, *ApJ*, 650, 604  
Riechers, D. A., et al. 2006b, *ApJ*, 645, L13  
Riechers, D. A., et al. 2007, *ApJ*, 666, 778  
Riechers, D. A., et al. 2008a, *ApJ*, 686, 851  
Riechers, D. A., Walter, F., Carilli, C. L., Bertoldi, F., & Momjian, E. 2008b, *ApJ*, 686, L9  
Riechers, D. A., et al. 2009, *ApJ*, 703, 1338  
Riechers, D. A., Carilli, C. L., Walter, F., & Momjian, E. 2010a, *ApJ*, 724, L153  
Riechers, D. A., Weiß, A., Walter, F., & Wagg, J. 2010b, *ApJ*, 725, 1032  
Riechers, D. A., et al. 2010c, *ApJ*, 720, L131  
Riechers, D. A. 2011a, *ASPC*, 446, 355  
Riechers, D. A. 2011b, *ApJ*, 730, 108  
Riechers, D. A., et al. 2011a, *ApJ*, 733, L12  
Riechers, D. A., et al. 2011b, *ApJ*, 726, 50  
Riechers, D. A., et al. 2011c, *ApJ*, 733, L11  
Riechers, D. A., Hodge, J., Walter, F., Carilli, C. L., & Bertoldi, F. 2011d, *ApJ*, 739, L31  
Riechers, D. A., et al. 2011e, *ApJ*, 739, L32  
Solomon, P. M., Rivolo, A. R., Barrett, J., & Yahil, A. 1987, *ApJ*, 319, 730  
Solomon, P., Vanden Bout, P., Carilli, C., & Guelin, M. 2003, *Nature*, 426, 636  
Solomon, P. M., & Vanden Bout, P. A. 2005, *ARA&A*, 43, 677  
Springel, V., et al. 2005, *Nature*, 435, 629  
Swinbank, A. M., et al. 2010, *Nature*, 464, 733  
Swinbank, A. M., et al. 2011, *ApJ*, 742, 11  
Tacconi, L. J., et al. 2008, *ApJ*, 680, 246  
Tacconi, L. J., et al. 2010, *Nature*, 463, 781  
Walter, F., et al. 2003, *Nature*, 424, 406  
Walter, F., et al. 2004, *ApJ*, 615, L17  
Wang, R., et al. 2010, *ApJ*, 714, 699  
Weiß, A., et al. 2007, *A&A*, 467, 955  
Wilson, C. D., Scoville, N., Madden, S. C., & Charmandaris, V. 2003, *ApJ*, 599, 1049